

Nanometer-Resolved Interfacial Fluidity

Richard C. Bell, Hanfu Wang, Martin J. Iedema, and James P. Cowin*

Contribution from the Pacific Northwest National Laboratory, P.O. Box 999, M/S K8-88, Richland, Washington 99352

Received October 29, 2002; E-mail: jp.cowin@pnl.gov

Abstract: Confined liquids can have properties that are poorly predicted from bulk parameters. We resolve with 0.5 nm resolution the nanoscale perturbations that interfaces cause on fluidity, in thin 3-methylpentane (3MP) films. The films of glassy 3MP are much less viscous at the vacuum-liquid interface and much more viscous at the 3MP-metal interface, compared to the bulk of the film. We find that the viscosity at the interfaces continuously returns to the bulk value over about a 3 nm distance. The amorphous 3MP films are constructed using molecular beam epitaxy on a Pt(111) substrate at low temperatures (<30 K). Ions are gently inserted at specific distances from the substrate with a 1 eV hydronium (D_3O^+) or Cs^+ ion beam. The voltage across the film, which is directly proportional to the position of the ions within the film, is monitored electrostatically as the film is heated at a rate of 0.2 K/s. Above the bulk glass transition temperature (T_g) of 3MP (77 K), the ions are expected to begin to move down through the film. However, ion movement is observed at temperatures as low as 50 K near the vacuum interface, well below the bulk T_g . The fitted kinetics predict that at 85 K, the glass is about 6 orders of magnitude less viscous near the free interface compared to that of the bulk.

I. Introduction

Fluids in highly confined spaces are increasingly seen as having properties that can differ markedly from that of the bulk fluid (see review 1). This can be profoundly important, as nanometer fluids are common in biological systems (e.g., ion channels), in heterogeneous chemistry (e.g., solution chemistry occurring in nanometer powders or zeolite-like structures), or in some nanoscale devices being dreamt up in labs across the globe.² Even a bulk fluid has interfaces, and if the properties of the fluid are strongly altered in the nanometer region of the interface, then this could strongly alter the interfacial transfer kinetics or the fluids' success as a lubricant or adhesive.^{3,4} Properties commonly believed to be altered at the interfaces of a fluid are the viscosity, molecular density, and ordering.

One issue in confined liquids is whether their properties are perturbed (a) uniformly across the entire confined liquid, or (b) vary on a molecular scale with an increase in the strength of perturbation as one approaches the interface.⁵ In the case of fluidity, we can draw analogies to traffic flow on a highway. A uniform change in fluidity across the entire film is like changing the highway's gross speed limit. Alternatively, a certain fluidity-enhancing interface would induce a kinetic "fast lane" adjacent to it, whereas another, stiffening interface would create a "slow

lane" next to it. Then as one moved away from the interface, the fluidity ("speed limit") would gradually return to that of the bulk.

Resolving this question requires making measurements on the nanometer scale of fluidity. To do so, we used ions as atomic-scale falling ball viscometers. While using ion mobility to measure viscosity is far from new, our geometry control allows unique insight into the rapid changes in fluidity near interfaces. To relate ion motion to viscosity, we make use of the Stokes–Einstein relation for the laminar fluid drag on a sphere, with minor modifications.^{6–7} This simplistic approach often works surprising well to describe the transport properties of ions through thin films. Researchers studying the fluidity of ultrathin or confined liquids¹ have relied on the Stokes–Einstein laws' validity to infer large changes from the bulk viscosity value, based on their observed change in friction or other kinetic data. The changes in fluidity that we report here are much larger than the expected deviations of the Stokes–Einstein law, as discussed.

The glass transition temperature T_g is the temperature near where the substance passes from the supercooled (or viscous) liquid state into a solid glassy state.⁸ T_g is commonly defined as the temperature at which the viscosity reaches 10^{13} poise, whereupon the liquid is "frozen" on the time scale of experimental observation, yet is still not crystalline. This viscosity is sufficient to slow even a single molecular rotation or atomic

(1) Granick, S. *Phys. Today* **1999**, *52*, 26–31.
(2) Burns, M. A.; Johnson, B. N.; Brahmaandra, S. N.; Handique, K.; Webster, J. R.; Krishnan, M.; Sammarco, T. S.; Man, P. N.; Jones, D.; Heldsinger, D.; Mastrangelo, C. H.; Burke, D. T. *Science* **1998**, *282*, 484–487.
(3) *Physics of Polymer Surfaces and Interfaces*; Sanchez, I. C., Ed.; Butterworth-Heinemann: Boston, 1992.
(4) Bhushan, B.; Israelachvili, J. N.; Landman, U. *Nature* **1995**, *374*, 607–616.
(5) Ge, S.; Pu, Y.; Zhang, W.; Rafailovich, M.; Sokolov, J.; Buenaviaje, C.; Buckmaster, R.; Overney, R. M. *Phys. Rev. Lett.* **2000**, *85*, 2340–2343.

(6) Bell, R. C.; Wu, K.; Iedema, M. J.; Cowin, J. P. *Hydronium Ion Motion in Nanometer 3-methylpentane Films*, submitted.
(7) Wu, K.; Iedema, M. J.; Schenter, G. K.; Cowin, J. P. *J. Phys. Chem. B* **2001**, *105*, 2483–2498.
(8) Ediger, M. D.; Angell, C. A.; Nagel, S. R. *J. Phys. Chem.* **1996**, *100*, 13 200–13 212.

scale diffusion to many minutes. In these active areas of research, it has been demonstrated that the properties of materials in unique environments can be dramatically different from those of the bulk.^{9–10} Recently, the deviation of T_g of thin polymer films has received great attention. These studies have been conducted on supported films,^{11–15} free-standing films,¹⁶ and on glass-forming liquids confined in nanoscopic pores.^{17–18} These studies typically measure the fluid property averaged over the film, using features such as breaks or hysteresis in the thermal expansivity or heat capacity versus temperature. Thin polystyrene (PS) films supported on silicon substrates demonstrate a downward shift in T_g as the thickness of the film decreases below 40 nm.^{9,11} It was suggested that this decrease in T_g is caused by the presence of a liquidlike layer at the polymer–air interface.¹¹ This model was further validated using free-standing PS films, where it was observed that T_g decreases much more rapidly with decreasing film thickness.¹⁶

Some excellent evidence for solid–liquid interface-induced gross increases in viscosity and crystallinity comes from shear force measurements between two mica sheets, where approximately 0 to 10 layers of solvent are trapped.¹⁹ X-ray scattering studies on nonconducting, nonpolar and nonreactive substances have shown that these liquids display distinct ordering for 3–6 layers at this interface, which does not display a dependence on the thickness of the film. Thin polymer films can show strong interfacial perturbations at solid interfaces as the substrate composition is changed thereby altering the interaction between the polymer and substrate. For example, poly(methyl methacrylate) (PMMA) on gold demonstrated the same behavior discussed above, that is, a lowering of T_g with a decrease in film thickness. On the contrary, PMMA on SiO displayed a stiffening effect corresponding to an increase in T_g with decreasing film thickness.¹² This was explained by a proposed “dead layer” near the interface between the polymer and substrate. These types of studies on confined liquids have shown that a nonuniform variation of the liquid density leading to a more rigid layer at the solid substrate is due to induced (or enhanced) ordering into discrete liquid molecular layers brought about by the approach of the second surface.²⁰

These studies have failed to lessen the debate on the distance scales of interfacial effects on fluidity,²¹ even the existence of any interfacial effect is contested.^{5,22} The polymer studies discussed above have been limited to measuring the average effect over the entire film and are not able to probe the possible

position dependence of the local properties within these films. Using shear modulation force microscopy, where by a 20 nm sharp tip is vibrated transversally, while being immersed into liquids, Overney and co-workers have attempted to probe the spatial variation of fluidity.⁵ They nicely demonstrated some 10² s of nanometer resolution in probing vertically structured films, and used their technique to conclude that the polymer films they studied did not show strong interfacial perturbations.⁵ Two caveats on this conclusion. First, as pointed out by the authors, these studies did not eliminate the possibility of strong interfacial perturbations at distance scales smaller than 10 nm. Second, although the authors want the probe to be nonperturbative, the nanometer force microscope tip clearly introduces a new interface and on the same distance scale as the phenomena being studied.

Although many of these experiments have shown apparently contradictory results, these discrepancies probably result from the small length scale (<10 nm) from the interfaces over which these perturbations occur. Many of these studies lack adequate spatial resolution to be sensitive to perturbations in this range. Although the shear force experiments have admirable control over the thickness of the film, or depth of insertion of the probe (for the scanning version), they measure an average property of the film below them, and cannot depth profile the fluidity of a fixed thickness film. True nonperturbative probes with spatial resolution would help resolve this issue. Some techniques that meet these criteria are those of surface light scattering and reflectivity. However, even these studies have given seemingly contradictory results demonstrating both loosening and stiffening at both interfaces.^{20,23–25}

We devised a nonperturbative probe of the interfacial fluidity near the free and solid interfaces of thin films with 0.5 nm resolution. We used vapor deposited glassy films of 3-methylpentane (3MP), and monitored the temperature-dependent motion of probe ions inserted at known initial positions in the film. Their motion in the film, as forced by their self-generated electric field, provides a sensitive and spatially resolved probe of the interfacial fluidity. The range of viscosities we probe, a few orders of magnitude around 10⁵ poise, is in the high viscosity range that is highly temperature dependent (for most fluids), and relevant to, for example gels and biological fluids.^{26,27}

II. Experimental Details

A. Apparatus and Sample Preparation. The experiments were carried out in an ultrahigh vacuum apparatus with a base pressure of 2×10^{-10} Torr. Although the details of the experimental apparatus and procedures have been reported previously,^{6,28,29} a brief overview of the apparatus and methods used are reported herein. These experiments can be separated into three fundamental steps as schematically shown in Figure 1. First, the organic film is epitaxially deposited onto a 1 cm

(9) Kawana, S.; Jones, R. A. L. *Phys. Rev. E* **2001**, *63*, 021 501.

(10) Liu, C. Z.; Oppenheim, I. *Phys. Rev. E* **1996**, *53*, 799–802.

(11) Keddie, J. L.; Jones, R. A. L.; Cory, R. A. *Europhys. Lett.* **1994**, *27*, 59–64.

(12) Keddie, J. L.; Jones, R. A. L.; Cory, R. A. *Faraday Discuss.* **1994**, *98*, 219–230.

(13) Forrest, J. A.; Dalnoki-Veress, K.; Dutcher, J. R. *Phys. Rev. E* **1997**, *56*, 5705–5716.

(14) DeMaggio, G. B.; Frieze, W. E.; Gidley, D. W.; Zhu, M.; Hristov, H. A.; Yee, A. F. *Phys. Rev. Lett.* **1997**, *78*, 1524–1527.

(15) Fukao, K.; Miyamoto, Y. *Europhys. Lett.* **1999**, *46*, 649–654.

(16) Forrest, J. A.; Dalnoki-Veress, K.; Stevens, J. R.; Dutcher, J. R. *Phys. Rev. Lett.* **1996**, *77*, 2002–2005.

(17) Jackson, C. L.; McKenna, G. B. *J. Non-Cryst. Solids* **1991**, *131*, 221–224.

(18) Arndt, M.; Stannarius, R.; Groothues, H.; Hempel, E.; Kremer, F. *Phys. Rev. Lett.* **1997**, *79*, 2077–2080.

(19) Raviv, U.; Laurat, P.; Klein, J. *Nature* **2001**, *413*, 51–54.

(20) Yu, C.-J.; Richter, A. G.; Kmetko, J.; Dugan, S. W.; Datta, A.; Dutta, P. *Phys. Rev. E* **2001**, *63*, 021 205.

(21) Mansfield, K. F.; Theodorou, D. N. *Macromolecules* **1991**, *24*, 6283–6294.

(22) Pu, Y.; White, H.; Rafailovich, M. H.; Sokolov, J.; Patel, A.; White, C.; Wu, W.-L.; Zaitsev, V.; Schwarz, S. A. *Macromolecules* **2001**, *34*, 8518–8522.

(23) Seydel, T.; Madsen, A.; Tolan, M.; Grübel, G.; Press, W. *Phys. Rev. B* **2001**, *63*, 073 409.

(24) Dosch, H.; Lied, A.; Bilgram, J. H. *Surf. Sci.* **1995**, *327*, 145–164.

(25) Bollinne, C.; Stone, V. W.; Carlier, V.; Jonas, A. M. *Macromolecules* **1999**, *32*, 4719–4724.

(26) Frauenfelder, H.; Sligar, S. G.; Wolynes, P. G. *Science* **1991**, *254*, 1598–1603.

(27) Buitink, J.; Hemminga, M. A.; Hoekstra, F. A. *Biophys. J.* **1999**, *76*, 3315–3322.

(28) Biesecker, J. P.; Ellison, G. B.; Wang, H.; Iedema, M. J.; Tsekouras, A. A.; Cowin, J. P. *Rev. Sci. Instrum.* **1998**, *69*, 485–495.

(29) Tsekouras, A. A.; Iedema, M. J.; Ellison, G. B.; Cowin, J. P. *Int. J. Mass Spectrom. Ion Proc.* **1998**, *174*, 219–230.

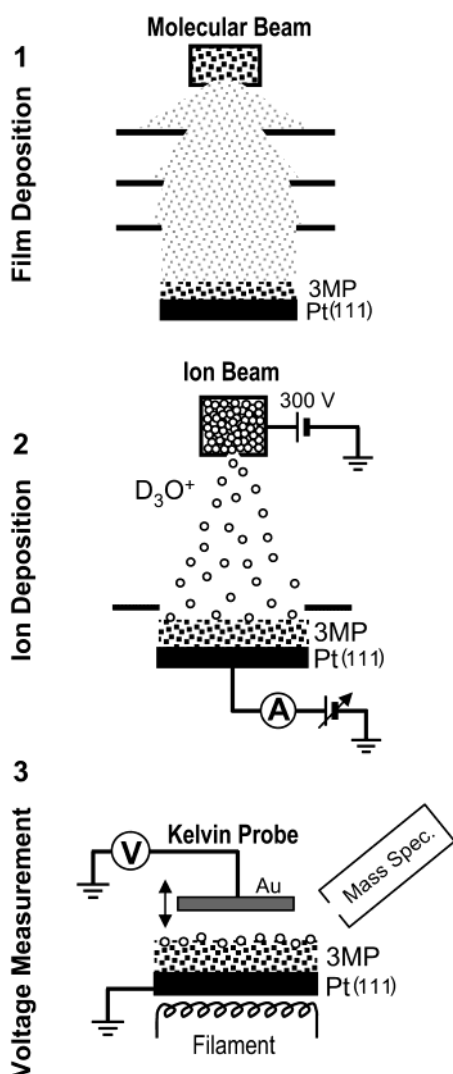


Figure 1. Experimental procedure. (1) 3-methylpentane is deposited at ~ 30 K as an amorphous layer. (2) Ions are deposited onto the film at approximately 1 eV as controlled by the bias difference between the ion source and the Pt crystal. Additional 3MP may be deposited on top of the ions to shield them from the free-interface. (3) The film voltage is electrostatically monitored and temperature programmed desorption spectra recorded as the temperature is increased at a constant rate (0.2 K/s).

diameter Pt(111) substrate using a 4-stage differentially pumped molecular beam. Second, hydronium (D_3O^+) or cesium (Cs^+) ions are gently deposited on the film. If ions are to be placed inside a film, then the film is deposited first to the thickness where the ions are to be placed, and then the ions are deposited. Finally, additional organic material is deposited on top, completing the film. The ions always have a kinetic energy at the target of less than 1 eV. Third, the voltage across the film, which is related to the average position of the ions within the film (further discussed below), is measured electrostatically and nonperturbatively using a Kelvin probe as the temperature is increased at a constant rate (0.2 K/s for these studies). These films begin to significantly evaporate starting around 120 to 140 K, above the temperature of all of the ion motion in these studies. This “thermal desorption” is monitored with a mass spectrometer.

The Pt(111) substrate was atomically cleaned via neon ion sputtering and annealing in 1×10^{-7} Torr oxygen to 1030 K and final annealing to 1200 K in a vacuum. Auger electron spectroscopy (AES) was employed to monitor surface cleanliness. The sample is cooled to below 30 K using a closed cycle He refrigerator and radiatively heated by an array of four W filaments located behind the substrate, capable of

heating the sample to temperatures in excess of 1200 K. The temperature is measured by a K-type thermocouple (Ni–Cr/Ni–Al) spot-welded to the sides of the sample. The films are grown on the substrate with submonolayer accuracy using a differentially pumped molecular beam in which the beam flux is controlled by a high precision flowmeter. 3-Methylpentane (3MP) was chosen for these studies because it does not crystallize at any temperature under normal experimental conditions.³⁰ All 3MP films were grown below 30 K. Prior to use, the high purity 3MP was further purified by freeze–pump–thaw treatments, in addition to the use of molecular sieve for removal of possible water contamination. Finally, the purity of the vapor was checked with a mass spectrometer. The deposition rate of the molecular beam is established from the film thickness, which is determined using reflectance techniques,⁶ and the time required to deposit the film. The deposition rate used for these studies was 0.49 \AA/s . Under these conditions, 8.5 s is required to deposit the first monolayer. This was determined using thermal desorption studies to find the first complete desorption peak. All exposures/coverages are reported as multiples of this nominal monolayer (ML) (estimated at 2.6×10^{14} molecules/cm²). At all coverages, 3MP molecules appeared to have unit sticking probability at the surface. Reflectometry was used to determine the film thickness for thick films. From these studies, it is found that 4.2 \AA of 3MP is deposited for each 8.5 s of dose, that is, 4.2 \AA per our nominal ML.

A filament source is used to create D_3O^+ in the ion source chamber by bombardment of the D_2O vapor by electrons and subsequent collisions with neutral molecules. A thermionic button source³¹ is used to create Cs^+ . The ions are extracted and focused by electrostatic optics and deflectors through two 5° bends along the ion path. These bends and liquid nitrogen traps located in the extraction region (differentially pumped chamber immediately following the ion source region) and just prior to the UHV chamber are used to suppress neutral water contamination during ion deposition. A Wien filter (with perpendicular electric and magnetic fields) is used to mass select the ion of interest. Finally, the ions are decelerated as they pass a grounded double mesh located about 1 cm away from the sample. The deposition energy of the ions is regulated to about 1 eV by biasing the sample. During ion deposition, the current of the impinging ions is recorded. In this manner, the total charge can be calculated by integrating the ion current over the deposition period. The total ion coverage in this study was about 0.05% of the surface density of the Pt(111) substrate (1.5×10^{15} atoms/cm²). All ion depositions were carried out below 30 K in this study.

The ions create a voltage across the film, which is related to the position of the ions within the film. (During ion deposition, this growing voltage requires us to continuously change the sample bias to maintain 1 eV ion energy.) The organic film acts like an insulating, linear dielectric medium creating a planar capacitor where ion deposition acts to charge the capacitor. The capacitance of the system is $C = Q/V$, where V is the potential difference across the capacitor and Q is the total charge created by the ions. The capacitance is also $C = \epsilon_0 \epsilon A/L$, where ϵ_0 is the vacuum permittivity, ϵ is the dielectric constant of the medium within the capacitor, A is the area of either plate and L is the distance between the plates of the capacitor. Combining these two equations gives $V = QL/\epsilon_0 \epsilon A$. If the ions are distributed throughout the film, it can be shown (see ref 32) that this is still valid for a uniform composition film, if one replaces L with the average height of the ions from the metal substrate, $\langle z \rangle$. Therefore, the ions in the film create a change in the contact potential difference, $\Delta\phi$, of the combined metal and film assembly by an amount

$$\Delta\phi = -\frac{Q\langle z \rangle}{\epsilon_0 \epsilon A} = -\Delta V \quad (1)$$

(30) Finke, H. L.; Messerly, J. F. *J. Chem. Thermodyn.* **1973**, *5*, 247.

(31) HeatWave Labs, Inc., Watsonville, USA, CA 95076: Model 1139–01.

(32) Tsekouras, A. A.; Iedema, M. J.; Cowin, J. P. *J. Chem. Phys.* **1999**, *111*, 2222–2234.

where ΔV is defined as the voltage across the film, which we will refer to as the film voltage.

The film voltage of the system is measured using a McAllister Kevin probe³³ with a sensitivity and measurement error of several mV. As the sample is warmed at 0.2 K/s, the change in the film voltage of the entire system is monitored; thereby, the average position of the ions within the film is tracked. Mechanical vibration can cause substantial noise, so during the measurement the He refrigerator is turned off while the temperature is maintained by the heat capacity of a long copper rod connecting the refrigerator to the sample. The vacuum deposition very slightly and very reproducibly aligns the (barely) polar 3MP molecules when deposited well below its glass temperature, to create a weak electret or ferroelectric voltage across the film.^{6,34,35} This voltage (~ 8 mV/ML for deposition at 30 K) is removed completely if the film is preannealed to above the glass temperature. If not preannealed, this ferroelectric voltage disappears just above the glass temperature, and just before the bulk of the ion motions, when the latter is present. When possible, the ferroelectric effect is removed by annealing the film prior to ion deposition.⁶ For ion sandwiches, the 3MP below the ions is preannealed, but the 3MP added on top cannot be. In that case, identical films without the ions are created, to measure the small ferroelectric voltage changes of the unannealed caps. This voltage is subtracted from the case with ions present. Ion motion in annealed or nonannealed films appears identical, and the ferroelectric voltages, when present, are so reproducible, that they are easily recognized, and are easily subtracted off.⁶

B. Modeling Ion Motion. The temperature evolution of the film voltage directly measures the ion mobility. Because we also desire to infer from these data the viscosity of 3MP, we will model the ion motion expected for a given viscosity (and its dependence within the film). The ions move under the influence of an electric field, the gradient of the electrostatic potential, which has independent contributions from both a solvation potential and a collective potential, the latter scaling as the charge per unit area. The solvation potential is calculated with the Born model.^{7,36} This short-range interaction is due to each individual ion interacting with the i th interface at z_i , including the “image attraction” of an individual ion to the metal substrate. This produces a short-range repulsion from the vacuum interface and similar attraction to the metal interface. The collective electrostatic potential arises as each ion interacts with the other ions as well as the interfacial images of all the other ions. The collective field that the ions feel is rather planar. This is typical for ion/film combinations of this size, as in biological membrane/aqueous interfaces with imbedded ions.³⁷ We calculate the potential as the sum of a simple planar capacitor potential (approximately equal to the collective potential) plus the Born interfacial potential. The gradient of this potential gives the force on the ions.

To model the ions’ motion through the film, we calculate the time evolution of the ion distribution $\rho(z)$ of positive ions of charge nq_e using the diffusion equation with an added term to account for mobility within the electric field as follows

$$\frac{d\rho(z)}{dt} = \frac{d}{dz} D(z) \frac{d\rho(z)}{dz} - \frac{d(\mu(z)\rho(z)\vec{E}_z(z))}{dz} \quad (2)$$

The first part on the right side of the equation deals with the thermal random-walk motion of particles described by the diffusion coefficient, D , whereas the second term models the systematic drift motion driven by an external electric field described by the ion mobility, μ . In the

above equation, we permit the D and μ to vary with z position. The diffusion coefficient and the ion mobility are linked by the Einstein relation³⁸

$$D = \frac{\mu k_B T}{nq_e} \quad (3)$$

Equation 2 is numerically propagated in time by the implicit, matrix approach.³⁹ For computational purposes, the film is divided into 5000 to 10 000 slabs and time steps on the order of 0.1 s. We estimate the ion mobility from the calculated drift speed of the ion within the electric field and assume that the Stokes formula is accurate on the microscopic scale and at the interfaces. The mobility is determined as follows

$$\mu(t) = \mu(T(t)) \approx \frac{nq_e}{6\pi\eta(T(t))r_1} \quad (4)$$

where t is the time, $\mu(t)$ is the ion mobility, $\eta(T)$ is the temperature-dependent viscosity of the organic film, nq_e is the total ion charge and r_1 is the ion hydrodynamic radius. $T(t) = \beta t$, where β is the linear temperature-ramping rate (0.2 K/s in this study). The diffusion coefficient is determined in the same manner via the Stokes–Einstein equation.

C. Bulk Viscosity. This paper looks at the interfacially perturbed viscosity. The nonperturbed viscosity is that nominally of the bulk. It is important that we understand the bulk viscosity and how the ion mobility measures it, to clearly see the perturbations of it. The bulk (or nearly bulk) properties of 3MP measured via ion mobility are the main topics of ref 6, only the key aspects are discussed here.

The temperature dependence of the viscosity of most liquids near the glass transition temperature displays non-Arrhenius behavior and is often well fit by the Vogel–Tamman–Fucher (VTF) equation.^{40–42}

$$\eta(T) = A e^{-E_a/R(T-T_0)} \quad (5)$$

The literature viscosity data is shown in Figure 2.^{43–46} Like most glasses, the bulk viscosity of 3MP indeed shows marked deviations from a simple Arrhenius behavior, as well as some scatter in the data. Indeed over the full range of the data from 77.5 to 293 K, even the VTF equation cannot accurately fit the data. However, over the range crucial to this experiment, 77.5 to 120 K, the VTF form fits it within the range of scatter.

To test the ability of the bulk viscosity and model to predict the ion motion when it is “far removed” from the interfaces, we constructed films with ions initially far away from either the top or bottom of the film.⁶ An example of this can be seen in Figure 3 for a 200 ML 3MP film with ions deposited on top and an additional 50 ML of 3MP was deposited atop the ions to shield them from the vacuum interface (solid curve). As we show later, this is more than enough to shield the ions from the short-range effects of the vacuum interface. The ions will still traverse the bottom interfacial region and encounter the stiffening, but on the scale of the 200 ML film, the stiffening of the last few monolayers creates a negligible effect on the film voltage in the region shown. This perturbation is more evident for thinner films as will be made apparent later. This curve displays the change in film voltage, which is directly proportional to the average position of the ions within

(33) McAllister Technical Services, Coeur d’Alene, USA, ID 83815: Model 6500.

(34) Iedema, M. J.; Dresser, M. J.; Doering, D. L.; Rowland, J. B.; Hess, W. P.; Tsekouras, A. A.; Cowin, J. P. *J. Phys. Chem. B* **1998**, *102*, 9203–9214.

(35) Wu, K.; Iedema, M. J.; Tsekouras, A. A.; Cowin, J. P. *Nucl. Instrum. Methods Phys. Res. B* **1999**, *157*, 259–269.

(36) Born, M. *Z. Phys.* **1920**, *1*, 45–48.

(37) Peitzsch, R. M.; Eisenberg, M.; Sharp, K. A.; McLaughlin, S. *Biophys. J.* **1995**, *68*, 729–738.

(38) Atkins, P. W. *Physical Chemistry*, 4th ed.; W. H. Freeman and Company: New York, 1990; p 764.

(39) Incropera, F. P.; DeWitt, D. P. *Fundamentals of Heat and Mass Transfer*, 4th ed; John Wiley & Sons: New York, 1996.

(40) Vogel, H. *Phys. Z.* **1921**, *22*, 645–646.

(41) Tamman, G.; Hesse, G. *Z. Anorg. Allg. Chem.* **1926**, *156*, 245–257.

(42) Fulcher, G. S. *J. Am. Ceram. Soc.* **1925**, *8*, 339–355.

(43) von Salis, G. A.; Labhart, H. *J. Phys. Chem.* **1968**, *72*, 752–754.

(44) Ling, A. C.; Willard, J. E. *J. Phys. Chem.* **1968**, *72*, 1918–1923.

(45) (a) Wilson, W. L.; Mellon, P. F.; Berberian, J. G. *J. Chem. Phys.* **1982**, *76*, 2602–2605. (b) Baranek, M.; Breslin, M.; Berberian, J. G. *J. Non-Cryst. Solids.* **1994**, *172*, 223–228.

(46) Ruth, A. A.; Nickel, B.; Lesche, H. *Z. Phys. Chem.* **1992**, *175*, 91–108.

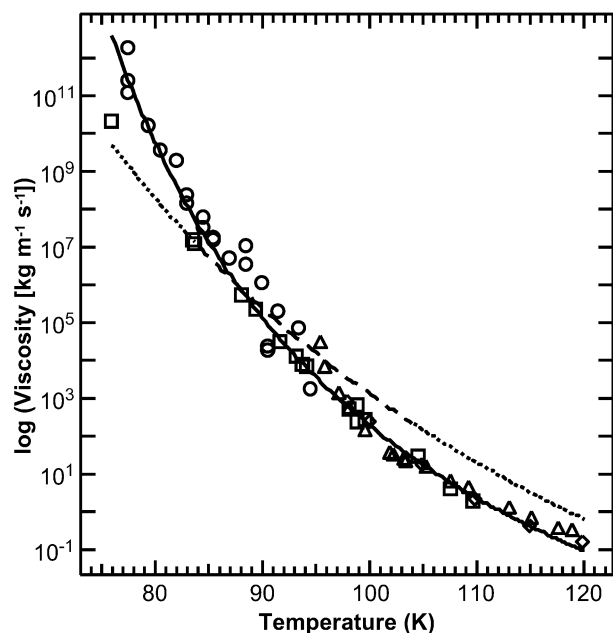


Figure 2. Solid curve is the fit of the viscosity of 3MP to the literature data of Labhart et al.⁴³ (triangles), Willard et al.⁴⁴ (circles), Berberian et al.⁴⁵ (squares) and Nickel et al.⁴⁶ (diamonds). The dashed curve represents the best fit of the viscosity to match the experimentally determined mobilities of D_3O^+ and Cs^+ in the bulk (central) portion of 25 to 2000 ML 3MP films. The parameters used for eq 5 for the literature fit are $A = 2.15 \times 10^{-10} \text{ kg m}^{-1} \text{ s}^{-1}$, $E_a/R = 1430 \text{ K}$, and $T_0 = 48.1 \text{ K}$ and for the fit to our experimental data are $A = 3.72 \times 10^{-16} \text{ kg m}^{-1} \text{ s}^{-1}$, $E_a/R = 3920 \text{ K}$, and $T_0 = 8.3 \text{ K}$. The dotted curve is the extrapolation of the dashed curve beyond the effective range of our measurements.

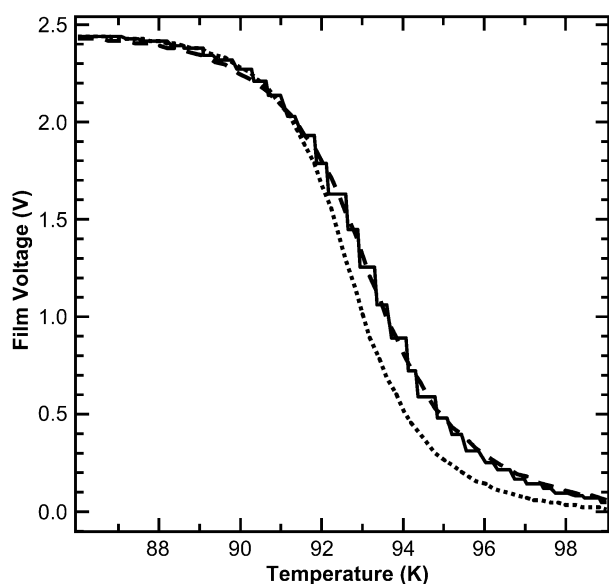


Figure 3. “Bulk” ion motion is shown, for a 200 ML (84 nm) 3MP film with ions deposited on top, followed by an additional 25 ML of 3MP deposited on the ions to shield them from interfacial effects. As the temperature of the film is increased at 0.2 K/s, the ions begin to move quickly through the film in the range of 88 to 98 K. This is evidenced by a drop in the film voltage. Modeling ion motion with Stokes Law using the literature value for the bulk viscosity of 3MP results in the dotted line. Note that this viscosity does not match the slope of the experimental curve. Therefore, an effective viscosity that matches our experimental data is used (Figure 2). Simulating the experimental data using this effective viscosity is shown as the dashed curve.

the film, as a function of temperature at a heating rate of 0.2 K/s. The dotted curve represents the ion motion modeled using eq 2 and the bulk viscosity of 3MP found in the literature (shown as the solid line

in Figure 2). An ion radius of 6 Å is used, representing one complete solvation shell. Note that although the simulation is quite similar to the experimental data, the simulated curve has too large of a magnitude of slope. This is typically true for all the film thicknesses that we have explored experimentally (up to 2000 ML of 3MP). Additionally, for a constant ion radius, the simulated ion motion will systematically drift away from the experiment, as the film thickness increases from 25 to 2000 ML, by about 2.2 K.⁶

These minor deviations involve likely one or several phenomena: long range (100 to 200 ML) small perturbations of fluidity, some residual effects of the buried interface that existed at the vacuum interface while the ions were deposited, a kinetic heterogeneity caused by the intrinsic nanometer-scale inhomogeneities for a glass near its glass temperature,^{47–48} or temperature-dependent deviations of the Stokes law from reality. As discussed in ref 6, several of these likely play a role, though modeling them is complicated. For simplicity in this paper, to adequately represent ion motion in the bulk regions of the film, we use an “effective viscosity” versus temperature,⁶ which varies somewhat more slowly than the best-fit data for the literature viscosity. This would be equivalent to assuming the ion radius was temperature dependent. This curve is shown in Figure 3, and fits the bulk ion motion well. It also fits the bulk ion motion in films from 25 to 2000 MLs of 3MP. Measuring the ion drop versus rate from 0.05 to 2 K/s verifies the *literature* viscosity;⁶ this effective viscosity is merely a convenient stand-in for more complex models. It does allow us to clearly notice the interfacial perturbations to the fluidity, which are much larger than the small effects discussed above.

III. Results

A typical measurement of the transport of D_3O^+ ions through a 25 ML (10.5 nm) 3MP film is shown in Figure 4. The experiments reported herein were repeated using Cs^+ ions, whose results were identical to those for the hydronium ions and are not shown. As the temperature of the film is ramped at 0.2 K/s, the ions begin to move quickly through the film in the range of 80 to 95 K as the viscosity of the 3MP quickly decreases (4 orders of magnitude in this range). This is evidenced by a drop in the film voltage (left axis), which is directly proportional to the average height of the ions within the film (right axis) as discussed previously. Below this temperature range, the high viscosity of the film allows little movement of the ions. For comparison, the dashed curve in this figure is that calculated using the continuum-based model given in eq 2 for the transport of ions with an assumed hydrodynamic radius of 6 Å (approximately one complete 3MP solvation shell) and calculated for a position-independent viscosity, that is, a constant bulk viscosity (the dashed curve in Figure 2) throughout the film. Although the simulation displays moderate agreement with the experimental spectrum, severe deviations are seen at both low and high temperatures. The bulk viscosity is much too high to permit any measurable ion motion at or below the glass transition temperature of 77 K, yet the experimental data shows substantial ion motion at or even below 77 K. On the other hand, at 95 K the bulk film viscosity is so low that theory predicts that all the ions should be at the bottom of the film, but the experimental data clearly shows that this is not yet the case. The vacuum interface displays a distinct loosening of the

(47) Ediger, M. D. *Annu. Rev. Phys. Chem.* **2000**, *51*, 99–128.

(48) Deschenes, L. A.; Vanden Bout, D. A. *Science* **2001**, *292*, 255–258.

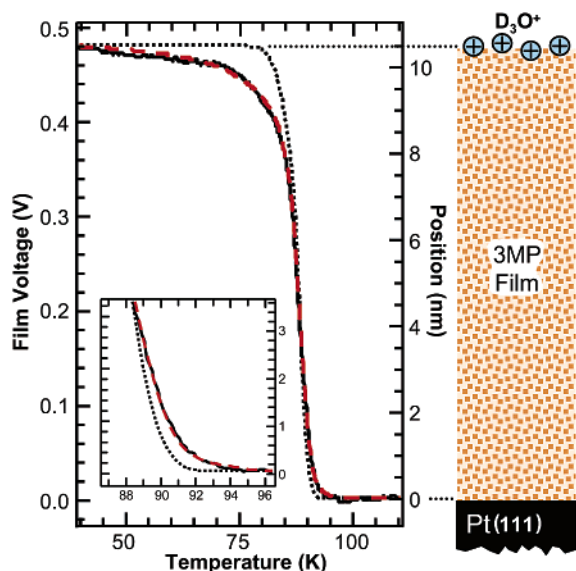


Figure 4. Typical spectrum for the transport of D_3O^+ ions through a 25 ML (10.5 nm) 3MP film is shown as the solid curve. As the temperature of the film is increased at 0.2 K/s, the ions begin to move quickly through the film in the range of 80 to 95 K as the viscosity of the 3MP quickly decreases (4 orders of magnitude in this range). This is evidenced by a drop in the film voltage (left axis), which is directly proportional to the average height of the ions within the film (right axis). The inset is an expanded view of the final ion motion near the 3MP–Pt interface. If the ions moved according to Stokes Law, then the bulk viscosity of 3MP would predict the dotted curve. The ions move near the top of the film more easily, and near the bottom of the film, less easily, than predicted by the bulk viscosity. The red dashed curve shows the predicted motion using our new position-dependent viscosity.

surface layers compared to the bulk, whereas a stiffening of the 3MP near the metal interface is observed.

To explore these deviations, sandwich films of 3MP/ions/3MP were constructed, where the bottom 3MP film was 25 ± 0.6 ML, and the thickness of the top 3MP film was varied. The ion motion (film voltage) as a function of temperature was monitored for each composite film as the top 3MP film thickness was increased, effectively increasing the ions' initial distance from the free interface. All films were created with an electric field of approximately 7.0 to 8.3×10^7 V/m and all curves are normalized to unity to accurately compare the position of the ions within the different films. After each run, the film voltage change as a function of temperature for films of identical thickness with no ions were collected using the same parameters. These spectra were then subtracted from the spectra of films containing ions to remove any voltage changes not due to ion movement.⁶ The bottom curve (labeled a) in Figure 5 displays the experimental results for a film with no shielding layers. As the number of shielding layers of 3MP is increased, the mobility of the ions is observed to approach that expected for a position-independent bulk film viscosity. At 7 ML (2.9 nm) or more of 3MP deposited on top of the ions, the interfacial effect is no longer observed and the curve is nearly identical to that predicted by the simple bulk viscosity.

The overall thickness of the film is increased by adding 3MP on top of the ions while maintaining a base of 25 ML of 3MP. This may induce changes in the film, independent of the ion position. Therefore, a second set of experiments was performed that maintained a constant film thickness, whereas the position of the ions within the film was changed. In addition, to avoid

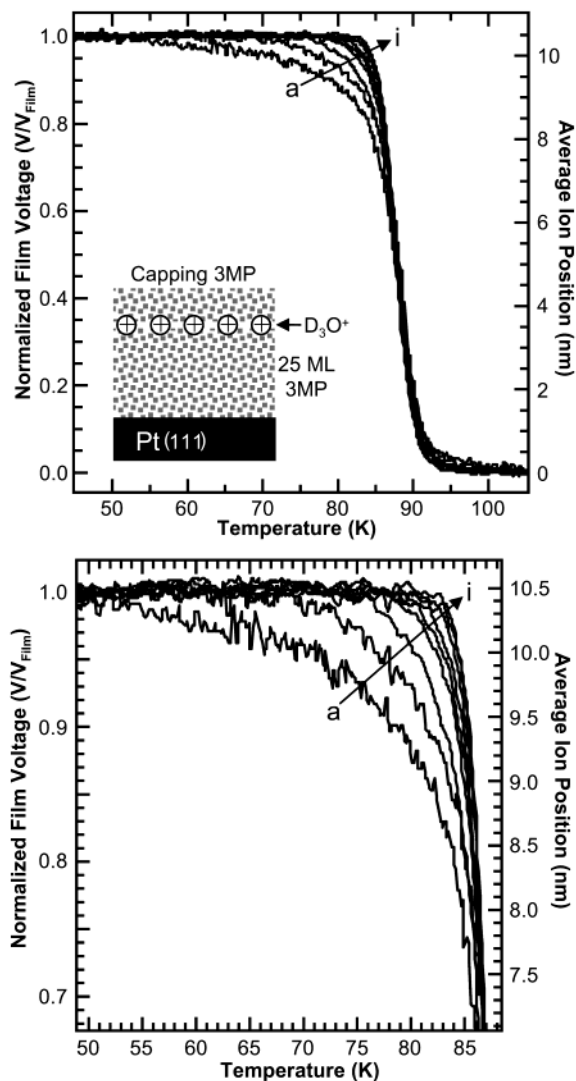


Figure 5. Normalized film voltage versus temperature curves for films where D_3O^+ ions are deposited 25 ML from the substrate. Further layers of 3MP are deposited on top of the ions to shield them from the free interface as shown for curves (a) through (i) representing 0, 1, 2, 3, 4, 5, 6, 7, 25 ML of 3MP deposited on top of the ions, respectively. All films have similar electric fields of $\sim 7 \times 10^7$ V/m. Noise within the experiments makes it difficult to simultaneously plot all the curves at once, to show the ion motion near the interface. Therefore, curves c through i have had a 0.9 K boxcar averaged smooth applied. The lower figure is the expanded area where the ions begin to move through the film.

the possibility of far reaching bottom effects due to interaction of the ions or solvent with the substrate, the thickness of the film was increased to 100 ± 2.5 ML (42 nm). An electric field of approximately 6.0 to 6.6×10^7 V/m was maintained throughout this series of experiments. As before, the ferroelectric background spectra of the film voltage changes as a function of temperature for films of identical thickness, but devoid of ions, were collected and subtracted from the data for films containing ions, ensuring that any change in film voltage is a result of ion movement. The interfacial effects for the constant thickness 100 ML films, shown in Figure 6, are nearly identical to those observed for the 25 ML bottom layer cases. Because all the films were created with the same electric field, the curves in this figure are all shifted along the y-axis to compare the position-dependent mobility of the ions as a function of their displacement from the vacuum interface. The bottom curve is

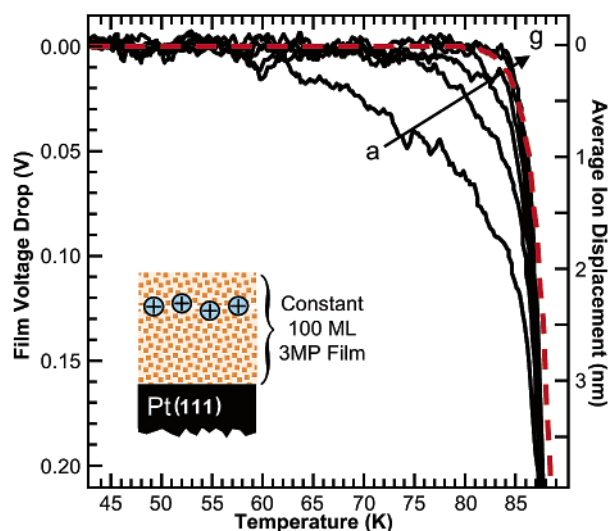


Figure 6. Film voltage versus temperature curves for constant 100 ML 3MP films with similar electric field of $\sim 6 \times 10^7$ V/m. Only the top portion of the curves (corresponding to the top 3.9 nm of the 42 nm thick film) have been shown, highlighting the area in which the change in ion mobility is observed. Noise within the experiments makes it difficult to simultaneously plot all the curves at once, to show the ion motion near the interface. Therefore, the curves have had a 1.5 K boxcar averaged smooth applied. Each of the curves (a) through (g) represents the initial position of the ions as they are deposited 0, 2, 4, 5, 6, 7, 30 ML, respectively, further into the film and away from the free-interface. The curves have all been shifted along the y-axis to enable comparison of D_3O^+ ion movement as a function of distance. The red dashed line is the voltage versus temperature curve predicted by the Stokes–Einstein model using the bulk film viscosity.

the case in which the ions are placed on top of the film. As the ions are moved further down into the film, away from the free surface, the curves again begin to approach that expected for the position-independent bulk viscosity shown here as the red dashed curve. With the ions moved 7 ML or more away from the interface, the ions have escaped the interfacial effects.

Other variations of this experiment confirm the short-range behavior of the interfacial fluidity shown above. For example, for ions on 100 ML 3MP films with 10 to 1000 ML of 3MP added on top (data not shown), the interfacial effects are identical to that shown in Figures 5 and 6.

IV. Discussion

The mobility of an ion moving through bulk 3MP would be expected to roughly follow the simple Stokes–Einstein equation, although deviations of an order of magnitude either way might be expected for a variety of reasons.⁶ An enormous increase in ion mobility is observed for the 3MP films at the vacuum–liquid interface, whereas a decrease in mobility is observed at the liquid–solid interface compared to that predicted by the bulk viscosity. The viscosity near the vacuum–interface at 85 K is found to be 6 orders of magnitude lower than that expected of a bulk film, as discussed later. We shall model the spatial changes in fluidity using Stokes law and an empirical fit of the data followed by some discussion of the possible causes of the perturbations at the free-interface.

Modeling Interfacial Position-Dependent Ion Motion. A large number of studies^{12,20,49,50} have shown that the physical

Table 1. Fitting Parameters for Modified VTF Equation

	A_i [K]	b_i [ML] (1 ML = 0.42 nm)
3MP–Pt interface term (1)	16.72	2.34
3MP–Pt interface term (2)	6.67	0.02
free-interface term (3)	19.66	1.45
free-interface term (4)	21.77	0.41

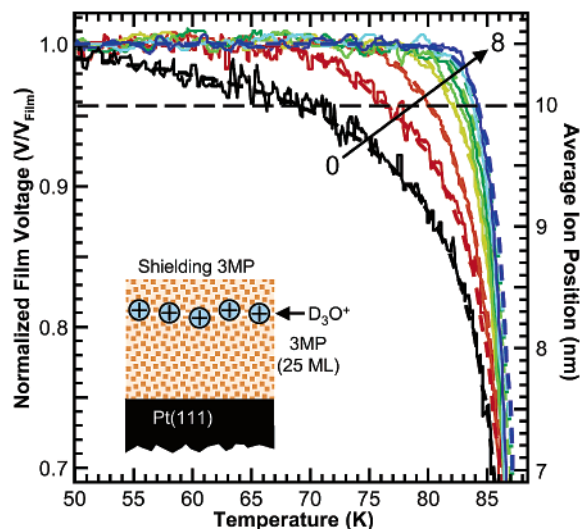


Figure 7. Comparison of experimental (solid) and simulated (dashed) normalized film voltage versus temperature curves display excellent agreement for any initial position of the ions within the film. Curves c through i have had a 0.9 K boxcar averaged smooth applied.

properties of liquids at interfaces often display strong perturbations from bulk behavior. In this study, we will model the perturbations as a position dependent viscosity. The structure of the ion diffusion equation (eq 5) already permits such a dependence. When D or μ do not depend on distance, they are typically placed outside the derivative. We modeled the viscosity of the film by letting T_g be a function of distance from the top and bottom interfaces, by modifying eq 5 to include an additional position-dependent term, $T_S(z)$, as follows

$$\eta(T, z) = Ae^{-E_a/R(T-T_0-T_S(z))} \quad (6)$$

T_S represents a shift in the glass-transition temperature

$$T_S(z) = (A_1e^{(-z/b_1)} + A_2e^{(-z/b_2)}) - (A_3e^{(-(L-z)/b_3)} + A_4e^{(-(L-z)/b_4}) \quad (7)$$

The thickness of the film is L and the distance the ions are from the bottom of the film is z . The A_x and b_x terms represent fitting parameters based on the experimental results (Table 1). The positive term gives stiffening near the Pt, and the negative term a loosening near the vacuum. It must be noted that we are not measuring the viscosity directly, but that the change in viscosity is inferred from the measurement of ion motion.

This function was used to fit the ion motion seen for a variety of initial ion positions and film thicknesses. As shown in Figures 4 and 7 for the 25 ML 3MP films, we get a very good fit to the observed ion motion. This results in an apparent decrease in T_g

(49) (a) van Zanten, J. H.; Wallace, W. E.; Wu, W. L. *Phys. Rev. E* **1996**, *53*, R2053–R2056. (b) Zheng, X.; Rafailovich, M. H.; Sololov, J.; Strzemechny, Y.; Schwarz, S. A.; Sauer, B. B.; Rubinstein, M. *Phys. Rev. Lett.* **1997**, *79*, 241–244.

(50) (a) Israelachvili, J. *Acc. Chem. Res.* **1987**, *20*, 415–421. (b) Heslot, F.; Fraysse, N.; Cazabat, A. M. *Nature* **1989**, *338*, 640. (c) Forcada, M. L.; Mate, C. M. *Nature* **1993**, *363*, 527.

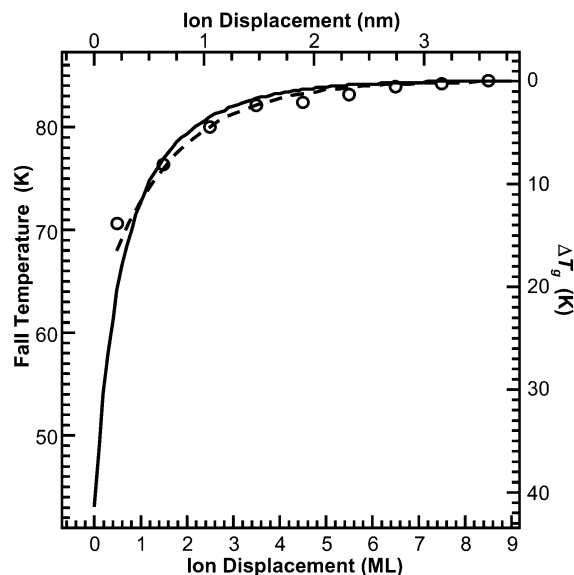


Figure 8. Spatial dependence of T_g at the free interface required to model ion motion in the films is shown as the apparent change in T_g versus distance from the free interface (solid curve, right axis). Also shown is the related property of the temperature at which the ions move a single monolayer as they are displaced farther from the free interface (left axis). The circles are taken from the data for the temperature ramping experiments, and shows the temperature at which an ion initially n monolayers away from the free interface moves (on average) to be $n + 1$ monolayers away (the temperature is taken at the position as shown by the dotted line in Figure 7) plotted against n . The dashed curve corresponds to extracting the n to $n + 1$ temperatures from the simulated ion motion. Both these values are plotted at the $n + 1/2$ position to display the excellent agreement between these values and the distance dependent shift in T_g .

as a function of distance from the interface as shown on the right-hand axis in Figure 8. As seen, this empirical fit of the position-dependent viscosity is found to reproduce the interfacial behavior of the ions either as they traverse the whole of a given film, or are initially placed progressively further into the film. We can use our fitted viscosity function, to estimate, at a fixed temperature, how much less viscous the top of the film is compared to the bulk. Using the parameters of Table 1, at 85 K the top of the 3MP film is 6 orders of magnitude less viscous than the bulk. This spatial dependence of the viscosity at 85 K, as inferred from the ion movement, is shown in Figure 9. Note that these measurements do not directly probe the dynamics near the interfaces at 85 K, as the ions generally are not located near the interfaces at this temperature. Instead, the viscosity at the interfaces is extrapolated from lower temperatures for the top, and from higher temperatures for the bottom of the film. The viscosity plotted in Figure 9 indeed shows a strong interfacial perturbation, and a clear indication of how poorly the estimate for ion motion would be using simply the bulk properties of the 3MP.

The model above, with a distance-dependent T_s , is not unique. In fact, we can fit all the data equally well using a position-dependent change in the activation energy in eq 6, including data versus ramp rate (see ref 6). The range of temperatures over which the ions move at any position that we can access is too small for us to distinguish an activation energy change from other changes in the kinetics.

Near the vacuum interface, because the film gets progressively more viscous as the ions move away from the vacuum, the

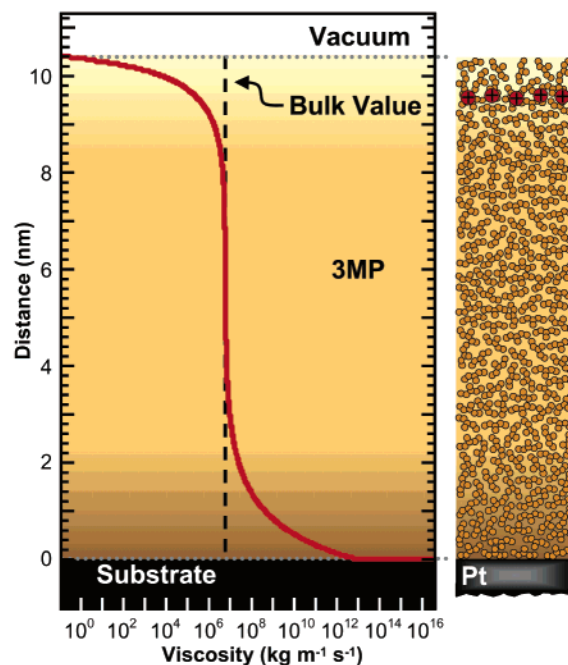


Figure 9. Spatial dependence of the viscosity at 85 K. The kinetics inferred from the ion motion are extrapolated using eqs 6 and 7 to show what predicted viscosity would be at a single temperature, 85 K.

position of the ions that initially started on the top of the film, should, during one of the temperature-ramped experiments, reflect the depth at which the viscosity has become too thick for movement at the current temperature. In this respect, the average ion position can give us sort of a direct measure of the intensive property of the fluid viscosity at the position represented by that voltage. Of course the ions do not move in a delta function band. They move with a very wide spatial distribution in homogeneous materials. But in fluids with a sharply increasing viscosity with depth, the ions (from our simulations) do move in a fairly tight band, and thus the initial changes in the average ion position (up to around 84 K) do correspond approximately to the fluid properties at a depth given by the drop in the film voltage. We can map the ion motion into a direct measure of the local viscosity at a particular temperature, even more directly by using the data where ions were placed at specific initial distances from the vacuum interface. In Figure 8, we plot the temperature at which ions initially n ML's from the top of the film manage to move to $n + 1$ ML's from the surface with the temperature being ramped at 0.2 K/s. This should represent the temperature at which the 3MP becomes fluid enough to allow 1 ML of ion motion in the time of a few seconds. This should shift precisely as does the glass temperature shifts. This is simply the temperature at the dotted line in Figure 7. Note that the change in the T_g curve in Figure 8 closely resembles the temperature curve at which ions move from n layers down to $n + 1$ in the 3MP film. Thus, we conclude that because the films become progressively stiffer as one goes further into the film, the ions will in general move inward until it becomes too rigid, and then wait until a rise in temperature permits additional motion.

Decreased Surface Fluidity at the Liquid–Solid Interface.

The present studies indicate that the mobility of the ions near the 3MP–Pt interface is slowed compared to the mobility

expected from the bulk film viscosity as seen in Figure 4. We have found that the stiffening near the 3MP–Pt interface appears to depend somewhat upon the cleanliness of the substrate surface. The cleanliness of the surface was monitored using AES, and it was found that even 1% of carbon surface contamination increases the nominal mobility of the ions near the Pt interface, shifting the bottom of the experimental curve by several degrees. The curves shown are for situations where we can be sure that the surface has less than 0.5% C or other contaminants. The fit for the thickening at the 3MP–Pt interface required a second exponential to represent a change that is restricted to largely the bottom monolayer of 3MP. The additional +12 K shift that occurs in the bottommost monolayer, probably reflects the strong binding of the first layer to the Pt, as evidenced by the thermal desorption of the bottom layer near 212 K, 82 K higher than the desorption of the next layer up.⁶

Given some shifting of the stiffening due to small amounts of surface contaminations and because as yet no experiments have been done inserting ions at known distances in the several nanometer region near the Pt interface, we do not as accurately know as much about the stiffening as we do about the loosening near the vacuum interface. We do get a good fit to the observed ion motion (with more scatter due to contamination shifts), using the parameters in Table 1. Interestingly, the exponential distance scale of the return to bulk behavior for either the stiffening or loosening are similar with values of 2.34 versus 1.45 ML, and with only a small (though noticeable) loss in fit quality, can be forced to a mean value around 2 ML. This should represent a distance scale over which the fluid recovers from any perturbation (of + or – sign), so it is comfortable that this is similar for both the top and bottom of the film.

Enhanced Surface Fluidity at the Vacuum–Liquid Interface. What is special about the surface that permits enhanced surface fluidity? As previously mentioned, studies of thin polystyrene (PS) films supported on hydrogen-passivated silicon substrates demonstrated that the glass transition temperature decreases with decreasing film thickness.^{9,11} It was proposed that the change in T_g is caused by the presence of a “liquidlike layer” at the free interface. Using ellipsometry to study the thermal expansivity of thin PS films, Kawana and Jones have estimated that the “liquidlike layer” penetrates approximately 10 nm into the film.⁹ Furthermore, the interfacial distance dependence of T_g does not appear to depend on the molecular weight of the PS films. The thickness of the “liquidlike layer” found for the polymer films is over 3 times the depth of 2.9 nm that we have found for the 3MP films.

The distance scale over which the interfacial effects persist (about 3 nm) should correspond to some natural distance for the liquid. Jagla and Tossatti,⁵¹ for example, predict a lowering of T_g near free interfaces, based on a formalism similar to one that predicts surface melting of solids. This would imply a strong temperature dependence to the distance scale of the viscosity changes. We have not incorporated such an idea in our model, nor as of yet have we optimized experiments to look for temperature dependent scale changes. This surface-enhanced fluidity could be caused by an increase in the vibrational amplitude of the interfacial molecules. On the basis of a simple model of a harmonic oscillator and pairwise forces between atoms, one might expect that surface vibrations are increased

due to the free surface. Molecules at the free-surface have fewer nearest neighbors as compared to those in the bulk and, therefore, within the context of a simple ball and spring model of a solid would experience less restoring force per unit displacement. Increased vibrational amplitudes at the free-interface have been observed both experimentally and theoretically for many bulk solids.^{52–54} The increased vibrational amplitudes have been shown to persist over 5 molecular layers into the surface⁵² (Note our 2.9 nm is around 7 molecules). The increase in vibrational motion of the molecules near the surface could cause an observed decrease in T_g . Another consequence of the free surface having fewer neighbors could lead to a greater ease for the vertical displacement of neutral molecules as the ions force their way down through the film, effectively increasing the fluidity at this interface. The results give a 12 K decrease in T_g one ML from the free surface. Fitting the data also requires an additional –29 K shift that occurs in the topmost monolayer. The additional loosening of the topmost layer could easily be an effect of film roughness, or related to the initial solvation of the ion in the film.

Yet another possible cause of the deviation in surface mobility could be due to a spatially heterogeneous fluid. Both theoretical and experimental studies have shown that supercooled molecular and polymeric glass formers can have a local structure and viscosity that is heterogeneous on a distance scale of 2 to 4 nm. These regions fluctuate over time.^{47,48} These studies have shown that the mobility can be drastically different in two regions of a fluid separated by only a few nanometers and that this dynamical heterogeneity grows as the temperature decreases toward T_g . They believe that this heterogeneity may arise from slight variations in density, local packing, or the “local energy landscape” and that these spatially heterogeneous dynamics are responsible for enhanced translational diffusion⁵⁵ compared to that predicted by the bulk viscosity. One implication of this is that we should be even more wary of the strict validity of the Stokes law and that this might account for the difference in slope between our effective bulk viscosity (dashed curve, Figure 2) and that observed using the more traditional methods of measurement (solid curve, Figure 2).⁶ We could also hypothesize that this tendency to spontaneously form internal structures should also create a sensitivity to the presence of an interface, and that they might define the natural distance scale for the propagation of an interfacial perturbation into the bulk. If the interfacial effects are mediated by this tendency to form heterogeneous regions, then the modeling of the ion motion (even in the bulk) may have to take explicit account of them.

We have considered, and largely discounted, other phenomena that could mimic or contribute to the interfacial ion mobility. Generally, liquids have thermally activated capillary waves. These dynamic fluctuations in the surface occur when the tendency of the surface tension to keep the surface flat is overcome by $k_B T$.⁵⁶ Precisely how this would affect ion motion is unclear. However, surface roughness due to the capillary wave

(51) Jagla, E. A.; Tosatti, E. *Europhys. Lett.* **2000**, *51*, 648–654.

(52) Allen, R. E.; de Wette, F. W.; Rahman, A. *Phys. Rev.* **1969**, *179*, 887–892.

(53) Reid, R. J. *Surf. Sci.* **1972**, *29*, 623.

(54) *The Chemical Physics of Solid Surfaces and Heterogeneous Catalysis*; King, D. A., Woodruff, D. P., Eds.; Elsevier: New York, 1981; Vol. 1, p 145.

(55) (a) Hall, D. B.; Deppe, D. D.; Hamilton, K. E.; Dhinojwala, A.; Torkelson, J. M. *J. Non-Cryst. Solids* **1998**, *235–237*, 48–56. (b) Chang, I.; Sillescu, H. *J. Phys. Chem. B* **1997**, *101*, 8794–8801.

(56) Penfold, J.; Thomas, R. K. *J. Phys.: Condens. Matter* **1990**, *2*, 1369–1412.

phenomena is unlikely to significantly contribute to our observed deviation from that expected for a bulk liquid for two reasons. First, capillary waves at room temperature display a root-mean-square roughness of 2 to 6 Å for water and other simple solvents,⁵⁷ far less than the 2.9 nm change that we observed. And second, the capillary wave phenomenon is temperature dependent where the width of the region affected by the capillary wave rapidly goes to zero near T_g .^{23,58} For example, recent studies on capillary wave dynamics on glycerol surfaces using X-ray photon correlation spectroscopy have demonstrated that the thermally activated capillary wave motion is essentially frozen by 44 K above the T_g of glycerol.²³

Another concern is the possibility that films deposited at very low temperatures can be initially surprisingly “fluffy” (i.e., expanded via internal voids) due to limited diffusion. This is particularly true for amorphous water.⁵⁹ If, upon warming, the film were to compact, this would have the dual effect of decreasing L and increasing ϵ , which from eq 1 would mimic ion motion. We have found that 3MP, unlike water, does not tend to make fluffy films at low temperature. A direct way to determine if the films deposited at low-temperature (<30 K) are or are not fluffy is to compare the ion motion of this type of film to one that has been preannealed well above T_g (>95 K and in excess of 5 min) before depositing ions. We have done this often, and repeatedly see no difference in the ion motion for films that are not annealed (with ferroelectric contributions subtracted by measuring the electrostatic changes without ions as a function of temperature), indicating that the 3MP films were not initially expanded, and therefore, structural relaxation leading to a change in free volume of the film is not the cause for the apparent change in interfacial viscosity.

Two other “topological” effects that might mimic an increase in surface fluidity are a film with a rough surface, due to random thickness fluctuations when growing the films, or roughness of the underlying Pt substrate. This might permit lateral surface diffusion of the ions to drop the film voltage, as the ions could seek out the thinner parts of the film. Surface roughness of the Pt is not likely an issue, as we observe identical enhanced surface fluidity in the top 2.9 nm for 25 to 1000 ML 3MP films, and independent of annealing treatments of the Pt(111) single-crystal substrate.

The possibility of grossly nonuniform molecular beam intensity was examined by isothermal temperature programmed desorption. This molecular beam has aperturing (including one aperture placed near the sample) designed to provide uniform-flat-topped dosing. Still it is important to test the design. To do so, we monitored the desorption of a thick multilayer film, using a mass spectrometer, while maintaining the film at a constant temperature where the evaporation rate is low. A flat film is expected to show a constant desorption rate (i.e., “zeroth order” desorption kinetics), followed by a sudden drop in the desorption rate as the last ML is desorbed. The desorption rate of an uneven film will drop off as the area of desorption changes (the appearance of areas of bare substrate caused by the complete desorption of thinner portions of the film).⁶ These studies

displayed a nearly constant desorption rate until the last 6.6% of the film desorbs. This indicates the film is globally very flat to within a few percent, over 97% of its area.

The Stokes–Einstein relation, which we use to theoretically calculate ion mobility, has been known to break down at high electric fields.^{60,61} We have explored ion motion across these films over a field range from 10^7 to 10^9 V/m for methylcyclohexane (MCH)^{7,35} and from 10^7 to 10^8 V/m for 3MP.⁶ These studies indicate that severe deviations from the normal shape of the curve begin to occur at fields of 1.5×10^8 V/m for both MCH and 3MP. The mechanism for this deviation is not well understood, though our results are in qualitative accord with pulsed ion mobility studies where severe deviations from the Stokes–Einstein relation for organics is observed for fields on the order of 10^8 V/m.⁶¹ The fields used in this study were maintained well below this high electric field threshold for nonlinear ion motion (in a range where we observe ion motion to be proportional to the electric field). Furthermore, if high fields were responsible, shielding the ions from the interface with more 3MP should not alter the motion of the ions through the film.

V. Conclusions

Our studies clearly indicate that ion mobility in thin organic films change dramatically near the liquid-vacuum interface. We are able to spatially resolve this fluidity with 0.5 nm resolution and show how nanometer films of glassy 3MP are much less viscous at the vacuum-interface than within the bulk of the film using ion mobility to probe the spatially varying flow properties. The ions begin to move at temperatures as low as 50 K near the vacuum interface, well below the bulk glass transition temperature of 3MP (77 K). The viscosity near the vacuum-interface at 85 K is found to be 6 orders of magnitude lower than that expected of a bulk film. With less precision, we see a similar stiffening at the 3MP–Pt interface. Furthermore, the fluidity perturbations were found to persist up to 2.9 nm into the film, which was determined by precisely placing the ions at increasing distances from the interfaces and monitoring the effect on the ion’s mobility. The data were very well fit using a position-dependent shift of the glass temperature of 3MP near its interfaces. It is still unclear as to the exact cause of the loosening of the free-interface, but is likely related to the typical softening of the phonon modes seen in most vacuum-solid interfaces.

Acknowledgment. This work was supported by the U.S. Department of Energy Office of Basic Energy Sciences, Chemical Sciences Division, and it was performed at the W. R. Wiley Environmental Molecular Sciences Laboratory, a national scientific user facility sponsored by the Department of Energy’s Office of Biological and Environmental Research and located at Pacific Northwest National Laboratory. Pacific Northwest National Laboratory is operated for the U.S. Department of Energy by Battelle under Contract DE-AC06-76RLO 1830.

JA0291437

(57) (a) Braslau, A.; Pershan, P. S.; Swislow, G.; Ocko, B. M.; Als-Nielsen, J. *Phys. Rev. A* **1988**, *38*, 2457–2470. (b) Braslau, A.; Deutsch, M.; Pershan, P. S.; Weiss, A. H.; Als-Nielsen, J.; Bohr, J. *Phys. Rev. Lett.* **1985**, *54*, 114–117.
(58) Jäckle, J.; Kawasaki, K.; *J. Phys.: Condens. Matter* **1995**, *7*, 4351–4358.
(59) Hessinger, J.; Pohl, R. O. *J. Non-Cryst. Solids* **1996**, *208*, 151–161.

(60) Debenedetti, P. G. *Metastable Liquids—Concepts and Principles*; Princeton University Press: New Jersey, 1996.
(61) Gosse, J. P. Electric Conduction in Dielectric Liquids. In *The Liquid State and Its Electrical Properties*; Kunhardt, E. E., Christophorou, L. G., Luessen, L. H., Eds.; Plenum Press: New York, 1988; p 503–508.